frontiers | Frontiers in Physics

TYPE Original Research
PUBLISHED 19 January 2023
DOI 10.3389/fphy.2023.1034157

OPEN ACCESS

EDITED BY
Xianfei Wen,
The University of Tennessee, Knoxville, United States

REVIEWED BY
Sushank Chaudhary,
Chulalongkorn University, Thailand
Erez Cohen,
Nuclear Research Center Negev, Israel

*CORRESPONDENCE
Quanhu Zhang,
zhangqh_102@sina.com

SPECIALTY SECTION
This article was submitted to Radiation Detectors and Imaging, a section of the journal Frontiers in Physics

RECEIVED 01 September 2022
ACCEPTED 02 January 2023
PUBLISHED 19 January 2023

CITATION
Lu Y, Zhang Q, Yao Q and Wang Y (2023), Optimal design of the neutron multiplicity counter based on metaheuristic algorithm. *Front. Phys.* 11:1034157.
doi: 10.3389/fphy.2023.1034157

Optimal design of the neutron multiplicity counter based on metaheuristic algorithm

Yunfeng Lu, Quanhu Zhang*, Qingxu Yao and Yu Wang

Xi'an Research Institute of High Technology, Xi'an, Shaanxi, China

The neutron multiplicity measurement and analysis method is a very important measurement and analysis method in the field of international arms control verification and nuclear safeguards, and its measurement accuracy depends to some extent on detector performance. In this paper, several newer current metaheuristic algorithms are introduced to achieve neutron multiplicity counter layout optimization by combining with MC (Monte Carlo) simulation software. The algorithm with the best finding ability is selected for the optimization of another detector layout. Based on the optimization results, k-means clustering analysis is introduced so that the optimized structure can be applied to neutron multiplicity measurements. The results show that the metaheuristic algorithm has good application capability for neutron detector layout optimization and can be further investigated.

KEYWORDS

neutron multiplicity, detector layout optimization, cluster analysis, MC simulation, metaheuristic algorithm

1 Introduction

Thermal neutron multiplicity counters are usually composed of a certain number of 3He tubes arranged uniformly in polyethylene, with different arrangements leading to different detection performances. Neutron multiplicity measurement is achieved by processing the neutron time information detected by the detector and solving the neutron multiplicity measurement equation to measure the mass properties of nuclear materials [1]. The current international 3He-based neutron multiplicity counters are AWCC [2], HLNCC (high-level neutron coincidence counting) [3], ENMC (epithermal neutron multiplicity counter) [4], etc. Different counters differ in the measurement layout and geometry, but each detector must consider layout optimization in its design. With a certain number of detector tubes, an algorithm is optimized to find the best layout to improve detection efficiency.

The production of 3He gas has been decreasing in recent years, but the demand for neutron detectors has increased substantially [5], the cost of neutron multiplicity counters based on 3He orthogonal counters has increased significantly, and research to replace 3He detectors is ongoing [6]. In the design of neutron multiplicity counters, the design of detectors needs to be reconsidered as new detectors become available.

The main difficulty of the current research on the optimization of the neutron multiplicity layout is that the counter usually contains multiple detector tubes. These detector tubes can produce an infinite variety of permutations, and it is difficult to abstract the process of detector's particle detection into a concrete mathematical formulation. Wang Duan et al. of the China University of Nuclear Technology introduced artificial intelligence methods to the optimization of the AWCC layout and initially realized the intelligent optimization design of the neutron multiplicity layout [7]. Using neural network prediction instead of the Monte Carlo (MC)

simulation process, the computational speed is greatly improved, but the accuracy is sacrificed to some extent. In recent years, with the rapid development of computer disciplines, methods for solving multi-objective optimization problems represented by metaheuristic algorithms are gradually enriched and have significant advantages in solving multi-objective problems and are well used in different disciplines. In this paper, we study the principle of neutron multiplicity counter detection and introduce a combination of the metaheuristic algorithm and MC simulation to find the optimal detection layout of the detector. The main contribution is the introduction of metaheuristic algorithm effectively combined with the MC procedure, applied to the field of neutron multiplicity counters, which provides new ideas for the detector design and makes the future design of neutron multiplicity counters more convenient and efficient.

The algorithm simulation of the article was performed in MATLAB 2021; the computer needs to install MCNP simulation software and the parallel program, and the processor is Inter Core i9-12900k.

2 Introduction to metaheuristic algorithm

A metaheuristic algorithm is an improvement of the heuristic algorithm with generality, which is a product of combining a random algorithm and a local search algorithm. Most of the current metaheuristic algorithms simulate the group hunting behavior of animals, and there are some differences between different algorithms but overall seem to have a similar idea of leading the whole population in a spatial search by a small number of good individuals. While traditional methods seem to struggle in the face of multi-objective optimization, metaheuristic algorithms can find near-optimal solutions quickly and have some engineering significance. In the metaheuristic algorithm, each population consists of several individuals, and the location of each individual constitutes a potential solution, and the optimal solution is finally obtained by continuously updating the location in a space. The disadvantages are that the operation is large, the operation time depends on the computer performance, and it may fall into local optima and cannot find the optimal solution in the real sense. Several well-developed metaheuristic algorithms in recent years are described in the following sections.

2.1 Gray wolf optimization algorithm

GWO (gray wolf optimization) algorithm was proposed in 2014 by Mirjalili et al. from Griffith University, Australia [8], and was developed based on the predatory behavior of gray wolf packs. A strict hierarchy is distinguished among gray wolf packs, and a small group of gray wolves with absolute leadership leads the whole pack in predation. Their ranks are α, β, δ, and ω from the top to the bottom, with gradually decreasing leadership power. The predation process is led by α wolves to complete, and there are three main processes: encirclement, pursuit, and attack. The gray wolf with optimal adaptation is considered the α wolf, the second best is the *ß* wolf, and the third best is the δ wolf in the simulation.

The process of encircling the prey is defined as follows:

$$X(t+1) = X_p(t+1) - A \cdot D, \tag{1}$$

$$D = \left|C \cdot X_p(t) - X(t)\right|, \tag{2}$$

where X denotes the position of the gray wolf, t denotes the number of current iterations, X_p denotes the position of the prey, and D denotes the distance between the gray wolf and the prey. The value of A simulates the behavior of the gray wolf. When A belongs to the interval $(-1, 1)$, the wolf attacks the prey, at which time the wolf falls into the local optimal solution. When not in the zone, the gray wolf moves away from its prey and explores other areas. C is a random weight between [0,2], which helps the wolf to avoid falling into a local optimum. A and C are calculated as follows:

$$A = 2a \cdot r_1 - a, \tag{3}$$

$$C = 2r_2, \tag{4}$$

where r_1 and r_2 are random numbers between [0,1] and a is linearly decreasing from 2 to 0 as the number of iterations changes. When the gray wolf identifies the prey location led by α, β, and δ and directs the whole wolf pack to pursue the prey, the mathematical model of the location update is described as follows:

$$X(t+1) = \frac{(X_1 + X_2 + X_3)}{3}, \tag{5}$$

$$X_1 = X_\alpha(t) - A_1 \cdot D_\alpha, \tag{6}$$

$$X_2 = X_\beta(t) - A_2 \cdot D_\beta, \tag{7}$$

$$X_3 = X_\delta(t) - A_3 \cdot D_\delta, \tag{8}$$

$$D_\alpha = |C_1 \cdot X_\alpha(t) - X(t)|, \tag{9}$$

$$D_\beta = \left|C_2 \cdot X_\beta(t) - X(t)\right|, \tag{10}$$

$$D_\delta = |C_3 \cdot X_\delta(t) - X(t)|, \tag{11}$$

where D_α, D_β, and D_δ denote the distance of each individual from α, β, and δ wolves, respectively; C_1, C_2, and C_3 are random numbers between [0,2]; X_α, X_β, and X_δ denote the current positions of α, β, and δ wolves, respectively; The position is updated for each individual using Eqs 5–11.

2.2 Whale optimization algorithm

WOA (whale optimization algorithm) was proposed in 2016 by Mirjalili et al [9]. Developed to simulate the hunting behavior of humpback whales, it uses a stochastic approach to simulate the hunting behavior and spirals to simulate the bubble attack behavior. Its search consists of three main processes: rounding up the prey, bubble-net predation, and searching for the prey.

The prey encirclement stage is to determine the location of the prey to facilitate the encirclement of the prey. As the iterative process increases, the location of the prey may change, requiring constant adjustment of the population location. The position update equation is as follows:

$$D = \left|C \cdot X_p(t) - X(t)\right|, \tag{12}$$

$$X(t+1) = X_p(t) - A \cdot D, \tag{13}$$

where t denotes the number of current iterations, $X_p(t)$ denotes the position of the global optimal whale, and $X(t)$ denotes the current whale position. A and C denote coefficients, and the formulas are consistent with GWO algorithm, as in Eqs 3, 4. Bubble-net predation involves swimming in a spiral shape toward the prey and constricting

the envelope. The two behaviors during the simulation are chosen according to probabilities, and the model is as follows:

$$X(t+1) = \begin{cases} X_p(t) \cdot D_1 \cdot e^{b1} \cdot \cos(2\pi l), p < P_i, \\ X_p(t) - A \cdot D, p \geq P_i, \end{cases} \tag{14}$$

where D_1 denotes the distance between the current individual and the current optimal individual, b denotes the spiral shape parameter, and l is a random number uniformly distributed between [−1, 1]. The mathematical model when searching for a prey is as follows:

$$D_2 = |C \cdot X_{rand}(t) - X(t)|, \tag{15}$$

$$X(t+1) = X_{rand}(t) - A \cdot D, \tag{16}$$

where D_2 denotes the distance between the current search individual and the random individual and $X_{rand}(t)$ denotes the position of the current random individual.

2.3 Sparrow search algorithm

SSA (sparrow search algorithm) was proposed in 2020 inspired by the foraging and anti-predatory behaviors of sparrows [10]. Sparrow populations are divided into discoverers, followers, and vigilantes. Discoverers are usually individuals with high energy reserves in the population and provide the area and direction for foraging for the whole population. The vigilantes move quickly to a safe area to get a better position once they realize the danger during the food search. The identity of the finder and follower changes dynamically throughout the search process, and any sparrow may become a finder as long as a better food source can be found.

During the food search, the discoverer's location was updated and expressed as follows:

$$X_{i,j}^{t+1} = \begin{cases} X_{i,j}^{t} \cdot \exp\left(-\dfrac{iter}{\alpha \cdot Max\_iter}\right), R_2 < ST, \\ X_{i,j}^{t} + Q \cdot L, R_2 \geq ST, \end{cases} \tag{17}$$

where $X_{i,j}$ shows the position information of the ith sparrow in the jth dimension, *iter* denotes the number of iterations, *Max_iter* denotes the maximum number of iterations, α is a random number between [0, 1], R_2 denotes the alert value, ST denotes the safety threshold, and Q is a random number obeying a positive-terrestrial distribution. L is a matrix with all 1's dimensions equal to the population dimension. When R_2<ST, it means that there are no natural enemies around and extensive foraging is possible.

The follower formula is updated as follows:

$$X_{i,j}^{t+1} = \begin{cases} Q \cdot \exp\left(\dfrac{X_{worst} - X_{i,j}^{t}}{iter^2}\right), iter > \dfrac{Max\_iter}{2}, \\ X_p^{t+1} + \left|X_{i,j} - X_p^{t+1}\right| \cdot A^{+}, otherwise, \end{cases} \tag{18}$$

where X_p denotes the optimal position of the current discoverer in the population and X_{worst} denotes the current global worst value.

Vigilante locations are updated as follows:

$$X_{i,j}^{t+1} = \begin{cases} X_{best}^{t} + \beta \cdot \left|X_{i,j}^{t} - X_{best}^{t}\right|, f_i > f_b, \\ X_{i,j}^{t} + K \cdot \left(\dfrac{\left|X_{i,j}^{t} - X_{worst}^{t}\right|}{(f_i - f_w) + \varepsilon}\right), f_i = f_b, \end{cases} \tag{19}$$

where X_{best} is the global optimal position. β is a step control parameter that obeys a positively random distribution of random numbers with mean 0 and variance 1. K is a random number between [−1, 1]. ε is a constant set to avoid a denominator of 0. f_i is the current fitness value of the individual sparrow. f_w and f_b are the current global worst and best values, respectively.

2.4 Hunger games algorithm

HGS (hunger games search) algorithm was designed in 2021 by animal hunger-driven activities and behaviors [11]. It is divided into proximity to food and hunger roles.

The animal approaching the food process is modeled as follows:

$$X(t+1) = \begin{cases} X(t) \cdot (1 + randn(1)), r_1 < 1, \\ W_1 X_b + RW_2 |X_b - X(t)|, r_1 > 1, r_2 > E, \\ W_1 X_b - RW_2 |X_b - X(t)|, r_1 > 1, r_2 < E, \end{cases} \tag{20}$$

where R is a random number of [−a, a]. r_1 and r_2 are random numbers between [0, 1]. t is the number of current iterations. W_1 and w_2 denote the hunger weights and are calculated as in Eqs 21, 22. X_b is the position where the current global optimum is located. E and R are calculated as in Eqs 23, 24.

$$W_1^i = \begin{cases} hungry(i) \dfrac{N}{Sum_{hungry}} r_4, r_3 < 1, \\ 1, r_3 > 1, \end{cases} \tag{21}$$

$$W_2^i = \left(1 - \exp\left(-\left|hungry(i) - Sum_{hungry}\right|\right)\right) \cdot r_2 \cdot 2, \tag{22}$$

$$E = \text{sech}\left(\left|f(i) - f_b\right|\right), \tag{23}$$

$$R = 2 \cdot a \cdot rand - a, \tag{24}$$

$$a = 2\left(1 - \frac{iter}{Max\_iter}\right), \tag{25}$$

where r_1, r_2, and r_3 are random numbers between [0, 1]. $f(i)$ denotes the fitness value of the ith individual. f_b is the current optimal fitness value. *sech* is a hyperbolic function, calculated as in Eq. 26. *Max_iter* and *iter* denote the maximum number of iterations and the current number of iterations, respectively. *hungry* denotes the hunger level of each individual, calculated as in Eq. 27. Sum_{hungry} denotes the sum of hunger of all individuals.

$$\text{sech}(x) = \frac{2}{e^x + e^{-x}}, \tag{26}$$

$$hungry(i) = \begin{cases} 0, fitness(i) = f_b, \\ hungry(i) + H, else, \end{cases} \tag{27}$$

where *fitness(i)* denotes the fitness value of each individual. H is calculated as follows:

$$H = \begin{cases} TH, TH \geq LH, \\ LH \cdot (1 + r), TH < LH, \end{cases} \tag{28}$$

$$TH = \frac{fitness(i) - f_b}{f_w - f_b} \cdot r_6 \cdot 2 \cdot (ub - lb), \tag{29}$$

where f_w and f_b denote the current global worst and optimal fitness values, respectively. u_b and l_b denote the upper and lower bounds of H, respectively. r_6 is a random number between [0, 1].

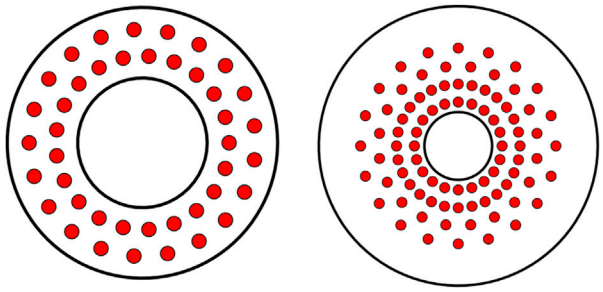

FIGURE 1
Schematic diagram of AWCC and NMC layout structures.

3 Principles and methods

3.1 Neutron multiplicity counting

Neutron multiplicity measurements have evolved from neutron coincidence counting. Compared with conventional neutron coincidence counting, which can only provide single and double count rates, multiplicity measurement can provide another parameter "triple" count rate for solving unknown parameters with high accuracy. Since nuclear materials emit a varying number of neutrons at the same time when they fission, the distribution patterns of different masses and types of nuclides are not the same; so, the mass properties of nuclear materials can be calculated based on the multiplicity distribution of fission neutrons. To improve this authentication capability, the triple count rate needs to be increased, and the counter layout design needs to be optimized to improve detection efficiency.

When nuclear material fissions, it randomly emits neutrons of different energies in all directions and loses energy by slowing down several times in polyethylene, increasing the probability of being captured by detectors as the energy continues to decrease. Once the neutrons are captured by 3He gas, a nuclear reaction occurs as in Eq. 30, generating charged particles and causing the detector to count them. Then, the neutron multiplicity shift register is used to process the neutron time information detected by the detector to generate the neutron multiplicity distribution, based on which the mass of nuclear material is calculated using the neutron multiplicity (Eq. 1).

$$n + {}^{3}He \rightarrow p + {}^{3}H + 764KeV. \tag{30}$$

3.2 Reference model

To facilitate comparative analysis, the AWCC [2] model of JCC-51 obtained from Canberra, United States, was studied to compare the optimization capabilities of different algorithms. Each 3He tube of the AWCC system has a length of 51 cm, a radius of 1.27 cm, an internal charge of 4 atm, a sample cavity radius of 8 cm, a 3.45-cm-thick cadmium reflective layer wrapped around the outside, and a detector with an outer boundary radius of 23.9 cm. The NMC-01 model was optimized by the algorithm with the strongest optimization capability and analyzed in comparison with the original structure. The NMC-01 was obtained from the 5RMC structure with an optimization improvement [12], with a sample cavity radius of 8.5 cm, a detector with an outer boundary radius of 35 cm, and an arrangement of 88 3He tubes, each 70 cm long and with a radius of 1.27 cm. The interior is filled with a charge of 6 atm. The layout of the two measurement systems is schematically shown in Figure 1, and the radius where each circle of detector tubes is located is shown in Table 1.

The optimization process in this paper is based on the aforementioned two detector models. In the model-building stage, some small structures are omitted, and for the layout optimization, the principle of control variables is used, and these omissions have almost no effect. During the optimization process, the measurement conditions are identical except for the detector tube arrangement position. The detection efficiency of both detectors, AWCC and NMC-01, was calibrated using a 3-mm-radius 252Cf source with results of 32.1% and 68.1%, respectively.

3.3 K-means clustering

K-means clustering algorithm is a typical division-based clustering algorithm, which is fast and simple to execute, and is widely used in the field of data processing [13]. The basic idea is to use a similarity measure to measure the relationship of all data in a dataset. First, the initial centers of k classes are selected, the distance of each sample point to these initial centers is calculated, and each point is divided to the center to which it belongs according to the distance, while the center of each class is recalculated. Then, each sample point is divided, and the process is repeated until the center of each class no longer changes.

3.4 General technical route

In this paper, the simulation is mainly composed of three parts: algorithm optimization, MCNP program simulation, and result processing, as shown in Figure 2. After determining the detector size, the detection model is established in MCNP. The model is then checked to make sure that there are no errors in the model and that the neutron multiplicity simulation can be performed. Since neutron multiplicity counters require the spatial detection efficiency curve to be as flat as possible, the detection tubes need to be symmetrically and uniformly distributed [14]. The optimization process transforms the coordinate information of the location of the detector tubes into a polar coordinate system to carry out improvement, where each tube corresponds to a uniform distribution of the pole angle, i.e., only the pole diameter needs to be considered in the optimization process. As for the AWCC structure, the polar angles of each tube differ by π/21. Since the location of the probe tube must be in the middle of the slowing agent, the polar diameter must lie in this interval when describing the upper and lower boundaries of the model. In addition, the detector tubes must not overlap with each other, i.e., the distance between the coordinates of the center of the detector tubes needs to be larger than the tube diameter. The simulated neutron source is a spherical 252Cf source with a radius of 3 mm, and the number of spontaneous fissions is set to 30,000, and 3,066 induced fissions occur, emitting a total of 125,849 neutrons.

TABLE 1 Radius of each circle of AWCC and NMC probe tubes.

	Model	First lap	Second lap	Third lap	Fourth lap
Radius/cm	AWCC	15.32	20.03	—	—
Radius/cm	NMC	11	15.5	20	24.5

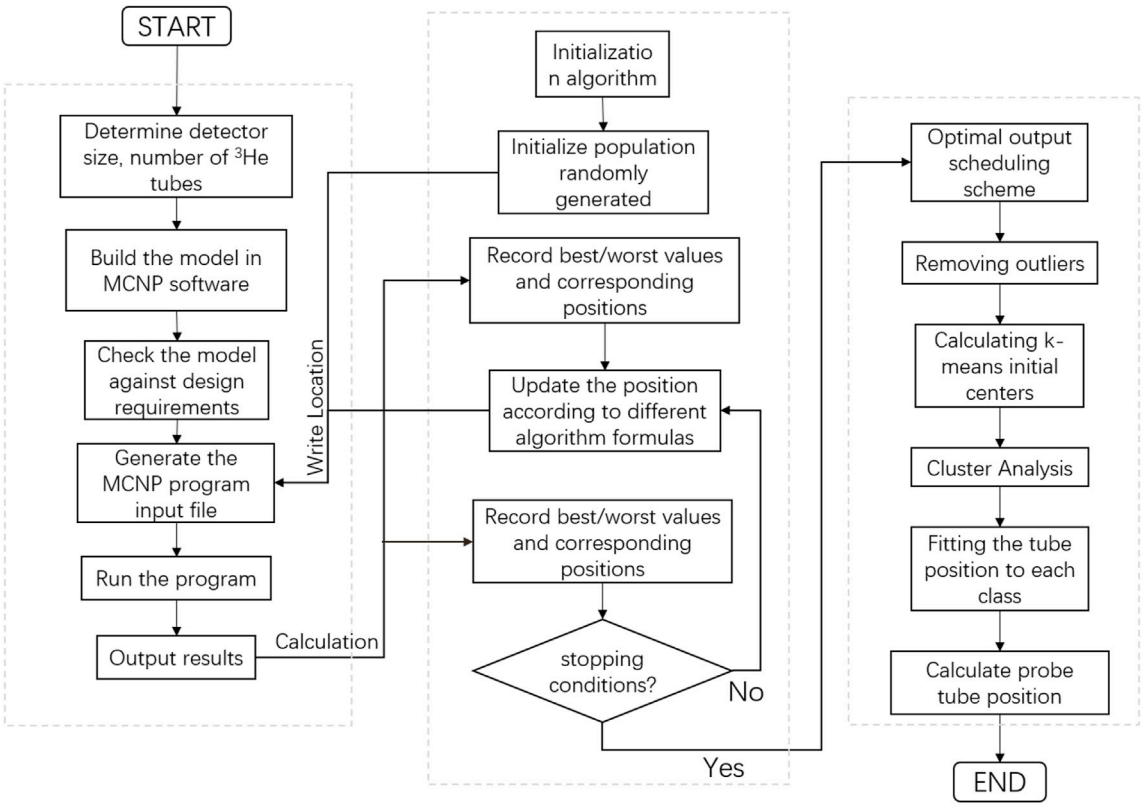

FIGURE 2
Flow chart of the general technical route.

In the optimization stage of the algorithm, the polar diameter sequence $[x_1,x_2,x_3... x_n]$ of all tubes for each probe layout constitutes individual X. To compare the optimization ability of different algorithms, the population size of each algorithm is specified as 30, and the number of iterations is 100. In addition, except for WOA, the smaller fitness value of the other algorithms represents the better position of the individual. The optimization algorithm requires a cost function to measure the fitness of the current position, but for neutron multiplicity counters, it is not possible to abstract each layout method with its corresponding detection efficiency into a concrete mathematical formula. Therefore, the algorithm needs to perform an MCNP simulation after each update of the location information to obtain the corresponding detection efficiency as an alternative to the cost function. At the same time, the metaheuristic algorithm relies on the generation of random numbers, and the results of the same algorithm run themselves differently. To observe the uncertainty and performance trends of the algorithms due to random numbers, the optimization process of each algorithm was repeated 10 times, and only the generated random numbers were changed during the repetition process, while the remaining parameters were kept consistent. In addition to this, the metaheuristic algorithm needs to process the position information beyond the boundary each time the position is updated. In this paper, we define that when the upper boundary is exceeded, it is forced to be equal to the upper boundary. When the lower boundary is exceeded, it is forced to be equal to the lower boundary. Also, any two tubes with a distance less than the tube diameter are subjected to random wandering with a variance of 3 and a mean of 0 until all constraints are satisfied.

The result processing stage is required to process the optimized layout because the layout optimized by the algorithm cannot strictly satisfy the uniform symmetric arrangement required by the neutron multiplicity counter. In this stage, the k-means cluster analysis method is introduced to distinguish the position information of different classes, and then the positions of each class are fitted to obtain the radius where each class is located.

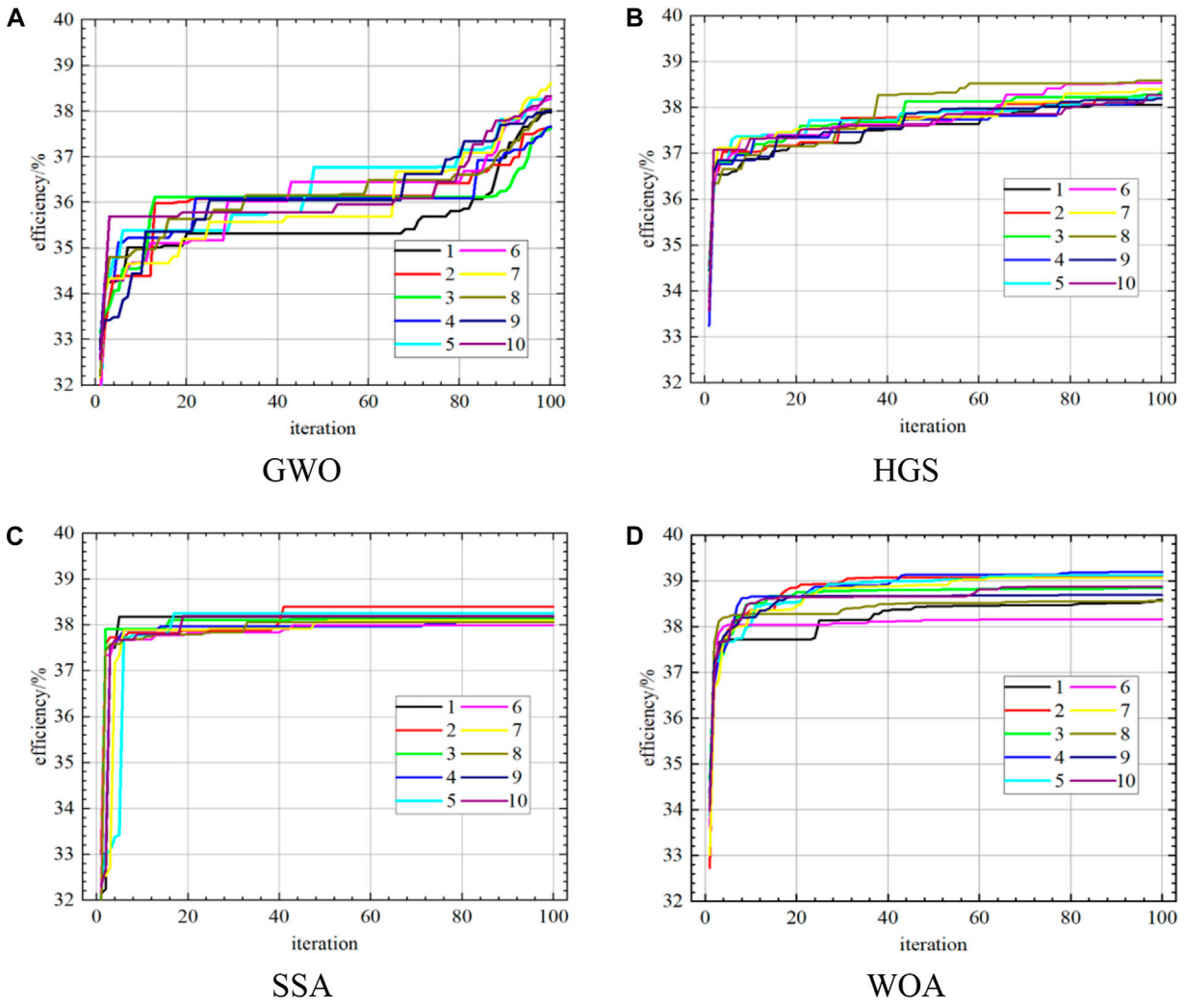

FIGURE 3
Trend of optimized detection efficiency of different algorithms.

4 Results and analysis

4.1 Analysis of AWCC optimization results

The trend of detection efficiency with the number of iterations in the optimization process of the four algorithms is plotted in Figure 3.

Figure 3 shows that the GWO, HGS, and search sparrow algorithms converge with close accuracy, and WOA converges with the highest accuracy. In terms of the convergence speed, WOA and SSA converge at almost the same speed, and GWO algorithm converges at the slowest speed. The average variation trend of the fitness value of each algorithm for 10 optimization processes is plotted in Figure 4. From the figure, it can be seen that WOA seems to be better than the other three algorithms both in terms of speed and performance, and it is more meaningful to study the optimization of the neutron multiplicity counter layout.

The layout of the AWCC detector for the 10 optimizations of the WOA is plotted in Figure 5. The first row from the left to the

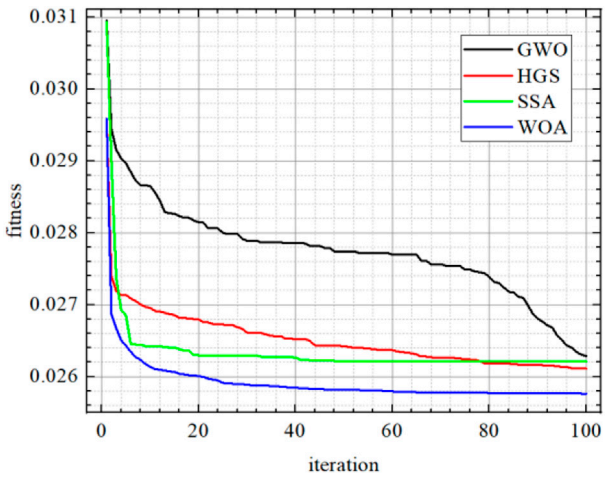

FIGURE 4
Trend of average adaptation of different algorithms.

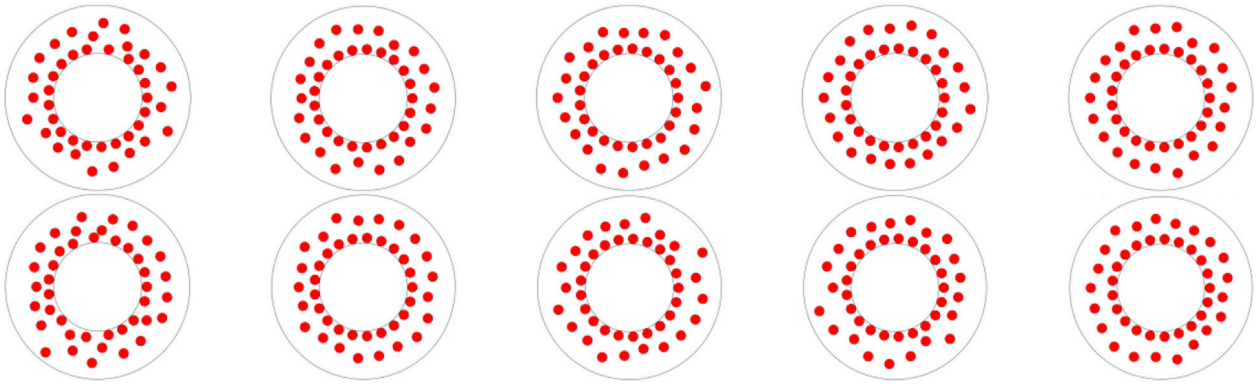

FIGURE 5
WOA to optimize the AWCC layout.

TABLE 2 Fitting the radius of the circle where each circle of the 10 layouts is located and the corresponding detection efficiency.

Layout	1	2	3	4	5	6	7	8	9	10
Inner ring/cm	12.89	12.75	12.79	12.75	12.77	13.27	12.75	12.76	13.11	13.15
Outer ring/cm	17.67	17.77	18.10	17.89	18.04	17.99	17.85	17.88	17.96	17.37
Efficiency/%	38.76	39.13	38.86	39.08	38.93	38.28	39.11	39.12	38.25	37.88

right shows the results of the first to the fifth optimizations, and the second row from the left to the right shows the results of the sixth to the tenth optimizations, respectively. As can be seen from the figure, the optimized layouts obtained each time are not the same, and there are some differences. This is because the algorithm approaches the optimal layout in different directions in the initial state generated randomly, and it is difficult to jump out of the local optimum after approaching a certain degree, which is an inherent defect of the metaheuristic algorithm. However, for neutron multiplicity counters, the detection structures need to be arranged uniformly and symmetrically to make the spatial detection efficiency within the sample cavity as flat as possible. The 10 optimized layouts can be seen to result in a roughly two-ring arrangement with approximately the same number of tubes in each ring. In order to optimize the layouts to be used for neutron multiplicity counting, the 10 layouts were clustered using k-means clustering algorithm, with category 2 selected, the initial centroids being the upper and lower limits of the detectors, respectively, and the number of iterations set to 500. The tubes of each of the two categories after clustering are fitted to a uniform circular arrangement to satisfy the symmetric design of the neutron multiplicity counter. The radii where the two circles of the fitted detection tubes are located and the corresponding detection efficiencies are shown in Table 2.

As can be seen from the table, the results obtained from the repeated runs are less different except for the sixth one, especially for the radius where the inner circle is located. Overall, the detection efficiency is almost around 39%, which is much higher than the 32.1% of the original layout. The generation of layout 6 is mainly due to the algorithm falling into a local optimum.

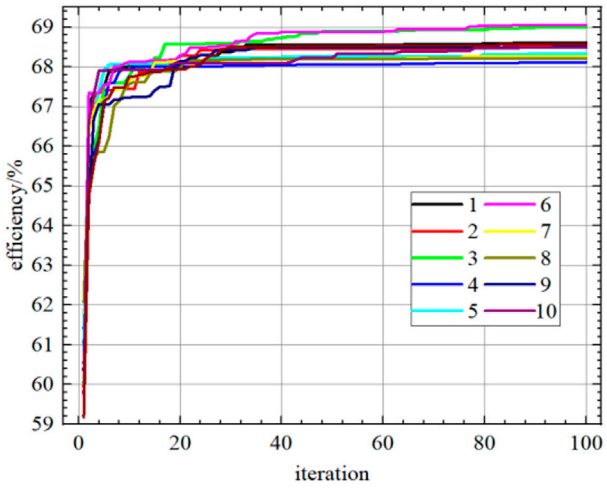

FIGURE 6
WOA-optimized NMC-01.

4.2 Analysis of NMC-01 optimization results

According to the final results of several algorithms, to optimize the AWCC layout, it seems that WOA optimization results meet the design requirements better. Here, the layout optimization of the NMC-01 model structure using WOA is theoretically much more complex due to the use of a larger number of 3He tubes. The NMC-01 detector structure itself is already an optimized structure, so the results of the optimization using WOA are compared with the original

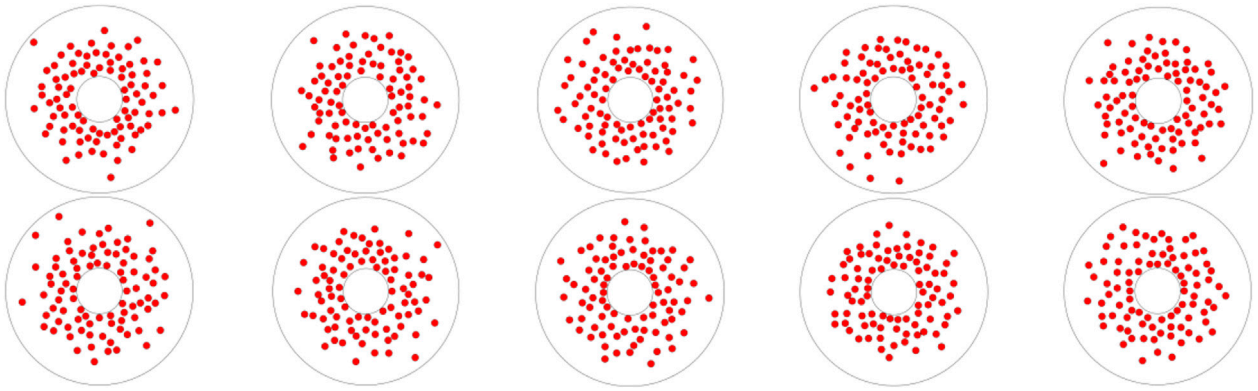

FIGURE 7
Optimal layout of NMC simulation 10 times.

TABLE 3 Radius of the circle in which each circle of the 10 layouts was fitted and the corresponding detection efficiency.

Layout	First lap		Second lap		Third lap		Fourth lap		Efficiency/%
	Radius	Pipe number	Radius	Pipe number	Radius	Pipe number	Radius	Pipe number	
1	10.81	16	14.37	25	18.95	30	24.74	17	69.71
2	10.45	15	14.05	20	18.24	27	23.97	26	70.23
3	10.92	20	15.07	25	19.29	22	24.88	21	69.96
4	10.64	19	15.48	29	21.26	34	27.26	6	69.24
5	10.67	18	14.31	19	18.65	32	24.24	19	69.89
6	10.34	17	14.93	27	20.32	33	26.96	11	69.32
7	10.63	18	15.33	27	19.71	28	25.69	15	69.79
8	10.39	19	14.90	23	18.87	23	24.41	23	69.83
9	10.73	19	14.30	19	18.01	25	22.97	25	69.65
10	10.58	19	14.77	23	19.91	29	24.69	17	69.91

detection efficiency to verify the ability of the application of the metaheuristic algorithm in the optimization of the neutron multiplicity counter layout. The variation in detection efficiency with the number of iterations is plotted in Figure 6.

As seen from the figure, the algorithm is able to converge quickly with each repeated run, and the converged detection efficiency is above 68%. The optimal layout obtained from 10 optimizations is plotted in Figure 7.

As can be seen from Figure 7, the greater the number of detection tubes used, the greater the difference in optimization results and the greater the gap with the neutron multiplicity counter design requirements. The same k-means cluster analysis method is used to classify the probe tube positions in the aforementioned layout into different classes in polar coordinates, as the initial centroid selection of the method has a large impact on the clustering results, and the selection of different initial centroids affects the clustering performance [15]. The number of classes selected is also very important; when the number is small, the number of inner circle probes is too much and will lead to an overlap of probes in the same circle. When the number of classes is chosen, the overlap between two circles may occur. It needs to be selected according to the actual situation, and this paper finds that NMC-01 meets various requirements when the number of corresponding selection classes is 4.

Since there is no specific method for the selection of the initial center point, this paper first finds the average of all tube center positions under one layout, calculates its distance from the detector cavity, and uses half of this distance as an increment to accumulate from the lower boundary of the detector tube. The radius where each circle of the final clustering is located and the number of tubes in each circle are shown in Table 3, the corresponding layout is plotted as shown in Figure 8, and the detection efficiency under this layout is simulated using MCNP. The final result has a certain improvement in detection efficiency compared with the directly optimized layout and meets the neutron multiplicity counter design requirements.

The results show that there is a certain difference in the final optimized layout, but the corresponding detection efficiency is not

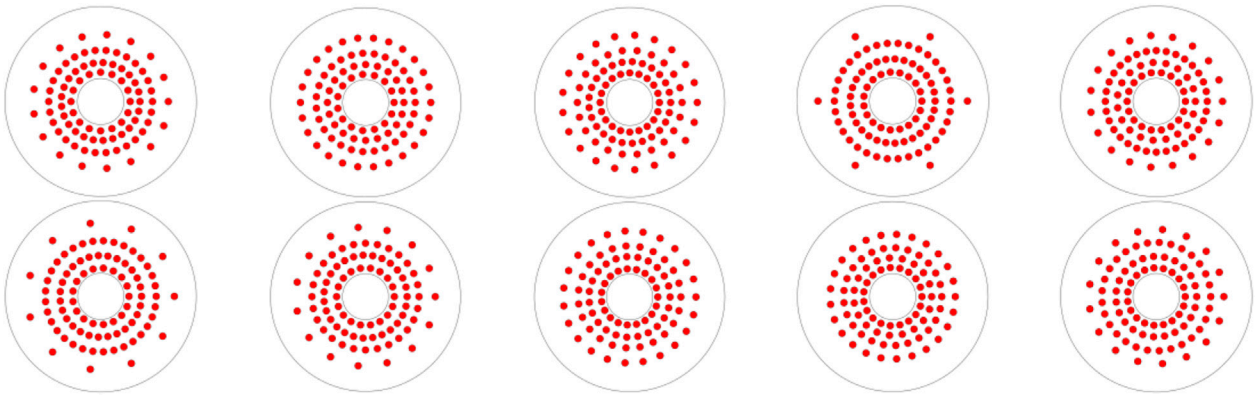

FIGURE 8
Optimal layout after NMC fitting.

very different. This is because the greater the number of detection tubes, the lower the proportion of each tube's contribution to the overall detection efficiency; a slight adjustment to the position of some of the detection tubes in the final layout will hardly affect the detection efficiency. Since this paper mainly focuses on this aspect of detection efficiency, no other parameters of the layout are required, but for neutron multiplicity counters, other factors need to be further considered. In addition, it can be seen from Figure 3 and Figure 6 that the algorithm has the largest trend of detection efficiency change in the early stage of layout optimization, and the algorithm can quickly converge near the optimal layout, and the sensitivity of the algorithm appears to be low at the later stage.

5 Conclusion

For the optimization of the neutron multiplicity detector layout, this paper introduces the metaheuristic algorithm combined with MCNP simulation to achieve fast optimization of the detection layout. According to the results of the optimization of the AWCC model and the NMC-01 model, it seems that the detection efficiency of the optimized layout is improved compared with the original layout after the introduction of the metaheuristic algorithm, thanks to the advantages of the metaheuristic algorithm in solving multi-objective problems. Therefore, this paper solves the problem of layout arrangement in the detector design to a certain extent and provides a new idea for the detector design. Although the algorithm in this paper can quickly optimize the layout, it can still be further improved. Due to the limitation to the metaheuristic algorithm itself, the algorithm may fall into a local optimum, so optimizing the same detector several times and selecting the optimal value can solve the problem to some extent. The algorithm design ideas need to be improved if we want to further improve the algorithm's optimal-seeking ability. In addition, k-means clustering algorithm also relies on the selection of the initial centroid, and the selection of a suitable initial centroid can also improve the final results to some extent. In general, the method proposed in this paper can meet the current multiplicity counter design requirements to a certain extent and has research value.

Data availability statement

The datasets presented in this study can be found in online repositories. The names of the repository/repositories and accession number(s) can be found in the article/Supplementary Material.

Author contributions

YL and YW performed the analysis. YL validated the analysis and drafted the manuscript. QZ reviewed the manuscript. QY and YL designed the research. All authors have read and approved the content of the manuscript.

Conflict of interest

The authors declare that the research was conducted in the absence of any commercial or financial relationships that could be construed as a potential conflict of interest.

Publisher's note

References

1. Langner DG, Stewart JE, Pickrell MM, Krick MS, Ensslin N, Harker WC, et al. *Application guide to neutron multiplicity counting*. Los Alamos, NM: Los Alamos National Laboratory (1998).

2. Canberra. Model JCC-51 active well neutron coincidence counter. *Canberra Industries* (2005) C26253.

3. Geist WH. *Multiplicity counting*. Los Alamos: America (2015).

4. Stewart JE, Menlove HO, Mayo DR, Geist WH, Carrillo LA, Herrera GD, et al. *The ephithermal neutron multiplicity counter design and performance manual: More rapid plutonium and uranium inventory verifications by factors of 5-20*. office of scientific and technical information technical reports (2000).

5. Shea DA, Morgan D. *The helium-3 shortage: Supply, demand, and options for congress*. Washington, USA: LIBRARY OF CONGRESS WASHINGTON DC (2011).

6. McElroy RD. *^{3}He alternatives summary report*. Tennessee, USA: Oak Ridge National Laboratory (2015).

7. Wang D, Li D, Wei Z, Hou C, Lin H, Li D, et al. Application of artificial intelligence method in layout optimization of ^{3}He pipe in AWCC. *At Energ Sci Tech* (2021) 55(5):954.

8. Mirjalili S, Seyed Mohammad Mirjalili Mirjalili A, Lewis. A. Grey wolf optimizer. *Adv Eng Softw* (2014) 69:46–61. doi:10.1016/j.advengsoft.2013.12.007

9. Mirjalili S, Lewis A. The whale optimization algorithm. *Adv Eng Softw* (2016) 95. doi:10.1016/j.advengsoft.2016.01.008

10. Xue J, Shen B. A novel swarm intelligence optimization approach: Sparrow search algorithm. *Syst Sci Control Eng* (2020) 8(1):22–34. doi:10.1080/21642583.2019.1708830

11. Yang Y, Chen H Ali Asghar Heidari. Heidari AH, Gandomi. AH. Hunger games search: Visions, conception, implementation, deep analysis, perspectives, and towards performance shifts. *Expert Syst Appl* (2021) 177:114864. doi:10.1016/j.eswa.2021.114864

12. Xu XM. *Research on neutron multiplicity measurement technology*. Beijing, China: China Institute of Atomic Energy (2008).

13. Wang J, Su X. IEEE. p. 44–6.An improved K-Means clustering algorithmProceedings of the 2011 IEEE 3rd international conference on communication software and networksXi'an, ChinaMay 2011

14. Zuo W, Zhang Q, Zhuang L, Li SF, Hou SX, Zhu LQ, et al. Research on detection efficiency spatial distribution of neutron multiplicity counting detector. *Nucl Elect Detect Tech* (2017) 37(12):1223–8.

15. Zhu M, Wang W, Huang J. Improved initial cluster center selection in K-means clustering. *Eng Computations* (2014) 31(8). doi:10.1108/EC-11-2012-0288